Photochemistry and Photobiology, 2012, 88: 537–547

Phthalocyanine Thio-Pyridinium Derivatives as Antibacterial Photosensitizers†

Joana B. Pereira[1,2], Eliana F. A. Carvalho[1], Maria A. F. Faustino[1], Rosa Fernandes[3], Maria G. P. M. S. Neves[1], José A. S. Cavaleiro[1], Newton C. M. Gomes[2], Ângela Cunha[2], Adelaide Almeida*[2] and João P. C. Tomé*[1]

[1]Department of Chemistry and QOPNA, University of Aveiro, Aveiro, Portugal
[2]Department of Biology and CESAM, University of Aveiro, Aveiro, Portugal
[3]Faculty of Medicine, IBILI, University of Coimbra, Coimbra, Portugal

Received 3 December 2011, accepted 3 February 2012, DOI: 10.1111/j.1751-1097.2012.01113.x

ABSTRACT

This study describes the synthesis of three new tetra- and octa-thio-pyridinium phthalocyanine derivatives. PSs 3a and 4a were prepared from the tetramerization of phthalonitriles 1 and 2, respectively, whereas PS 5 was prepared from the nucleophilic substitution of the 8 beta fluor atoms of hexadecafluorophthalocyaninatozinc(II) by mercaptopyridine, followed by cationization. The recombinant bioluminescent *Escherichia coli* strain was used to assess, in real time, the photoinactivation efficiency of these cationic phthalocyanines, under white and red light. The cellular localization and uptake were also determined to assess the potential of the new phthalocyanines as antibacterial agents. Derivative 3a was the most effective PS, causing a 5 logs reduction in bioluminescence after 30 min of irradiation under white or red lights. The photoinactivation efficiency of the phthalocyanine 4a was similar (5 logs reduction in bioluminescence) to that of 3a when irradiated with white light, but the efficiency of inactivation was reduced (2.1 logs reduction in bioluminescence) under red light. The tetra-substituted phthalocyanine 3a also generates high amounts of singlet oxygen, does not aggregate in PBS and is highly fluorescent, which makes it an effective PS and a promising fluorescent labeling.

INTRODUCTION

The inappropriate prescription of antibiotics to treat infectious diseases, with the consequent development of antibiotic resistance among pathogenic bacteria was already recognized by the scientific community as a major emerging health care issue that needs urgent solutions (1). Bacterial replication is very fast, hence a mutation that allows their survival in the presence of a killing agent, such as an antibiotic drug, will rapidly become predominant, leading to microbial resistance (2). Therefore, alternatives to control microbial infections are needed and photodynamic therapy (PDT) is already considered an important and very promising one that in principle would not lead to microbial resistance (3–6).

Photodynamic therapy is based on the theory that a photoactivable compound, a PS, can be preferentially localized in certain cells/tissues and when activated by light of an appropriate wavelength, generates singlet oxygen and/or free radicals, which are cytotoxic to targeted cells (7). This approach presents several advantages compared with traditional antimicrobials, namely: (1) a short time of inactivation; (2) effectiveness independent of the antibiotic resistance profile; (3) nondevelopment of photoresistance after multiple treatments; (4) lack of mutagenicity; and (5) availability of broad spectrum PSs with a wide range of microbial targets (8).

Several studies showed that phthalocyanines are efficient in the photodynamic inactivation of both Gram-positive and -negative bacteria (9–13).

Phthalocyanines, considered second generation PSs in PDT, are macrocycles constituted by four isoindole units connected by four nitrogen atoms, forming an internal 16-membered ring, characterized with red wavelength absorption (>670 nm), long triplet lifetime ($\approx$1 ms) and good quantum yields of singlet oxygen generation ($\Phi_{\Delta ZnPc} = 0.56$ in DMF; 10,14,15). They can occur as metal-free phthalocyanines or metallophthalocyanines if the hydrogen atoms of the central cavity are replaced by a metal (16). These type of compounds tend to aggregate easily, which can compromise their photodynamic effect, but their water solubility can be enhanced through the use of adequate substituents in peripheral positions of the macrocycle (17,18). Zinc phthalocyanines have been studied as efficient drugs in microbial photodynamic inactivation (11–13,19,20) as well as in cancer PDT (21–23). A previous study showed that a tetra-substituted cationic Zn(II) *N*-methylpyridyloxy phthalocyanine at 10 μM induced a 4.5 log decrease of *E. coli* cell survival after a total light dose of 54 J·cm^{-2} delivered at the fluence rate of 30 mW·cm^{-2} of visible light (12). An octa-cationic Zn(II) phthalocyanine with four bis(*N*,*N*,*N*-trimethyl)amino-2-propyloxy groups, also showed an efficient photosensitizing effect against *E. coli* after irradiation with a diode laser operating at 200 mW·cm^{-2} for 5 min (11). Another study involving cationic substituted Zn(II) phthalocyanines, bearing anilinium groups in different positions, showed a *Staphylococcus aureus* survival decrease of

†This paper is part of the Symposium-in-Print on "Antimicrobial Photodynamic Therapy and Photoinactivation."

*Corresponding author emails: aalmeida@ua.pt (Adelaide Almeida); jtome@ua.pt (João P. C. Tomé)

≈4.6 log, without affecting fibroblasts, when a concentration of 0.1 μM and a total light dose of 15 J·cm^{-2} delivered at the fluence rate of 50 mW·cm^{-2} of red light was used (24). Regarding cancer PDT, Zn(II) phthalocyanine presented an efficient selectivity and photosensitization of MS-2 fibrosarcoma (21) and its liposome-incorporated preparation also affected drastically cell survival of tumorigenic non- and highly metastic transformed rat fibroblasts (22). Plus, a liposomal preparation of zinc phthalocyanine (CGP55847) has undergone clinical trials (Phase I/II, Switzerland) against squamous cell carcinomas of the upper aerodigestive tract (23). Thiol-substituted phthalocyanine complexes are known to absorb light at higher wavelengths (> 700 nm) and to present good photochemical and spectroscopic properties (25,26).

Although Gram-positive bacteria are generally susceptible to the most PS used in conventional PDT (27–29), a different situation is reported for the Gram-negative bacteria, that in general are insensitive to photodynamic effects in the presence of neutral or anionic PS (30–32). The different susceptibility to the photodynamic process between the two types of bacteria is due to structural differences on their cell wall. Although Gram-positive bacteria have a much thicker peptidoglycan layer than Gram-negative bacteria, their wall presents a rather high degree of porosity. On the hand, the cell wall of Gram-negative bacteria has an additional membrane layer, external to the peptidoglycan, that presents an asymmetric lipid structure composed by strong negatively charged lipopolysaccharides (30,33). The external membrane markedly decreases the bacterial permeability of Gram-negative bacteria. This constraint can be overcome by using cationic PS that can penetrate in cells by the self-promoted uptake pathway, through the interaction of the positive charges of the PS with negatively charged sites of the outer membrane, resulting in an increased permeability and consequently increase of susceptibility to the photodynamic effect (18,29,34–36).

The aim of this study was to evaluate and compare the photoinactivation efficiency of the new tetra and octa-thiopyridinium phthalocyanines **3a**–**5a** against Gram-negative bacteria. Similar tetra- and octa-substituted compounds were already produced in previous studies, but in very low yields (12%; 37,38). Herein, we describe a new and simple synthetic approach to prepare, in high yields, tetra- and octa-thiopyridinium phthalocyanines to test their potential as PS for Gram-negative bacteria. The photoinactivation efficiency of these cationic phthalocyanine derivatives was evaluated, in real time, using a bioluminescent *E. coli* strain as a model of Gram-negative pathogenic bacteria. The light and PS dose applied in this study were somewhat higher than the ones used in other studies to produce effective target cell destruction to facilitate the comparison among the different PSs.

MATERIALS AND METHODS

General methods. ^{1}H, ^{13}C and ^{19}F solution NMR spectra were analyzed on a BrukerAvance-300 spectrometer at 300.13, 75.47 and 282.38 MHz, respectively. $CDCl_3$ and DMSO-d_6 were used as solvents and tetramethylsilane (TMS) as internal reference; the chemical shifts are expressed in δ (ppm) and the coupling constants (J) in Hertz (Hz). Mass spectra were recorded on a MALDI-TOF/TOF 4800 Applied Biosystems. UV–Vis spectra were obtained on a Shimadzu UV-2501PC spectrophotometer. Column chromatography was carried out using silica gel (Merck; 35–70 mesh). All chemicals were supplied by Sigma–Aldrich. Solvents were purified or dried according to the literature procedures (39).

Synthesis of phthalocyanines and precursors. 4-Thiopyridylphthalonitrile 1. A dimethylformamide (DMF) (5 mL) solution of 4-nitrophthalonitrile (1.00 g, 5.78 mmol) and 4-mercaptopyridine (1.62 g, 1.44 mmol) was stirred at room temperature under a nitrogen atmosphere for 10 min. Dry potassium carbonate (214 mg, 1.5 mmol) was added and the mixture was heated at 50°C for 5 h. The residue was resuspended in water (80 mL) and extracted with ethyl acetate (three portions of 50 mL). The fraction containing the 4-thiopyridylphthalonitrile **1** was purified by recrystallization from dichloromethane, yielding 0.96 g (70%). mp: 146–148°C. ^{1}H NMR ($CDCl_3$): δ 7.35 (dd, J = 1.6 and 4.5, 2H, Py-*o*-H), 7.91 (dd, J = 1.8 and 8.2, 1H, H-5), 8.15 (d, J = 8.2, 1H, H-6), 8.28 (d, J = 1.8, 1H, H-3), 8.54 (dd, J = 1.6 and 4.5, 2H, Py-*m*-H). ^{13}C NMR ($CDCl_3$): δ 113.9, 115.4, 115.8, 116.1, 124.0, 134.9, 136.1, 136.2, 139.9, 143.8 and 150.5.

4,5-Dithiopyridylphthalonitrile 2. Dry potassium carbonate (0.5 g, 3.6 mmol) was added to a solution of 4-mercaptopyridine (0.677 g, 6.09 mmol) and 4,5-dichlorophthalonitrile (0.5 g, 2.5 mmol) in DMF (3 mL) in an ice bath and under a nitrogen atmosphere. The reaction was left at room temperature and nine more portions of dry potassium carbonate (50 mg each portion) were sequentially added every 10 min. After the last addition, the reaction was kept under stirring for 2 h more. Distilled water was added and the precipitate formed was filtered and purified by chromatography over a silica gel column using a mixture of CH_2Cl_2/MeOH (9:1) as eluent. The resulting product was recrystallized from CH_2Cl_2, yielding 0.60 g of **2** (50%) mp: 238–240°C. ^{1}H NMR ($CDCl_3$): δ 7.25 (dd, J = 1.5 and 4.5, 4H, Py-*o*-H), 7.57 (s, 2H, H-3,6), 8.67 (dd, J = 1.5 and 4.5, 4H, Py-*m*-H). ^{13}C NMR ($CDCl_3$): δ114.2, 114.8, 125.4, 135.0, 141.7, 142.6, 151.2. MS (ESI-TOF) *m/z*: 347 $[M+H]^+$.

$ZnPcH_{12}SPy_4$ 3. A mixture of phthalonitrile **1** (400 mg, 1.69 mmol) and zinc acetate (276 mg, 2.02 mmol) in dimethylaminoethanol (DMAE, 1.5 mL) was placed under reflux (140°C) for 15 h. After cooling to room temperature, the reaction mixture was washed with MeOH/H_2O (9:1) and the residue was filtered and washed with methanol. Metallophthalocyanine **3** was obtained in 82% yield (351 mg) after vacuum drying. mp: > 300°C. ^{1}H NMR (DMSO-d_6 + TFA): δ 7.79–7.92 (m, 8H, Py-*o*-H), 8.29–8.45 (m, 4H, Pc-β-H), 8.65–8.70 (m, 8H, Py-*m*-H), 8.90–9.45 (m, 8H, Pc-α-H). UV–Vis (DMSO) λ_{max} (log ε): 347 (4.98), 617 (4.55), 684 (5.37) nm. MS (MALDI-TOF) *m/z*: 1013.07 $[M+H]^+$.

$ZnPcH_8SPy_8$ 4. A mixture of phthalonitrile **2** (285 mg, 0.82 mmol) and zinc acetate (138 mg, 1.01 mmol) in DMAE (1 mL) was placed under reflux (140°C) for 15 h. After cooling to room temperature, the reaction mixture was washed with MeOH/H_2O (9:1) and the residue was filtered and washed with methanol. The product **4** was dried under vacuum, yielding 254 mg (85%). mp: > 300°C. ^{1}H NMR (DMSO-d_6 + TFA): δ 8.02 (d, J = 6.0, 16H, Py-*o*-H), 8.70 (d, J = 6.0, 16H, Py-*m*-H), 10.15 (s, 8H, Pc-α-H). UV–Vis (DMSO-d_6) λ_{max} (log ε): 371 (4.59), 632 (4.47), 663 (4.68), 702 (5.03) nm. HRMS (MALDI-TOF) *m/z*: calcd for $C_{72}H_{40}N_{16}S_8Zn$ ($[M]^+$) 1448.0673, found 1448.0643.

$ZnPcF_8SPy_8$ 5. DEA (5.0 mL) was added to a DMF (50 mL) solution of **$ZnPcF_{16}$** (200 mg, 0.23 mmol) and 4-mercaptopyridine (205 mg, 1.85 mmol) and the reaction mixture was kept under stirring at room temperature for 24 under N_2 atmosphere. After this period, the DMF was evaporated under vacuum and the resulting product was washed with acetone. The desired derivative **5** was obtained in 89% (328 mg) yield after crystallization from water/acetone. mp: > 300°C. ^{1}H NMR (DMSO-d_6): δ 7.28 (br s, 16H, Py-*o*-H), 8.19 (br s, 16H, Py-*m*-H). ^{19}F NMR (DMSO-d_6): δ−126.7 and −127.2 (2s, 8F, Pc-α-F). UV–Vis (DMSO) λ_{max} (log ε): 384 (4.82), 690 (5.04), 720 (5.09) nm. HRMS (MALDI-TOF) *m/z*: calcd for $C_{72}H_{33}F_8N_{16}S_8Zn$ 1592.9998 ($[M+H]^+$), found 1592.9927.

Methylation of metallophthalocyanines 3–5. A large excess of methyl iodide (4 mL) was added to a stirred solution (or suspension) of metallophthalocyanines **3**–**5** (100 mg) in dry DMF (20 mL). The reaction mixture was heated at 40°C overnight in a sealed tube. The reaction mixture was cooled in an ice bath and the cationic phthalocyanines were precipitated with diethyl ether, filtered and washed several times with diethyl ether. The solid was dissolved in acetone/H_2O (1:1) and reprecipitated with acetone. The products were dried under reduced pressure and obtained in quantitative yields.

ZnPcH$_{12}$(SPyMe)$_4$ 3a – mp: >300°C. ^{1}H NMR (DMSO-d_6): δ 4.21 (4s, 12H, CH_3), 7.87–7.99 (m, 8H, Py-*o*-H), 8.35–8.51 (m, 4H, Pc-β-H), 8.67–8.74 (m, 8H, Py-*m*-H), 9.30 (br s, 8H, Pc-α-H). UV–Vis (DMSO): λ_{max} (log ε): 352 (4.60), 616 (4.39), 685 (5.20) nm. MS (MALDI-TOF) *m/z*: 1027.10 $[M\text{-}3CH_3]^+$.

ZnPcH$_8$SPyMe$_8$ 4a – mp: >300°C. ^{1}H NMR (DMSO-d_6): δ 4.23 (s, 24H, CH_3), 8.10 (d, J = 7.1, 16H, Py-*o*-H), 8.72 (d, J = 7.1, 16H, Py-*m*-H), 10.15 (s, 8H, Pc-α-H). ^{13}C NMR (DMSO-d_6): δ 46.9, 122.9, 133.1, 133.5, 141.2, 144.5, 153.4, 160.8. UV–Vis (DMSO) λ_{max} (log ε): 383 (4.55), 630 (4.38), 702 (5.03) nm. MS (MALDI-TOF) *m/z*: 1463.0 $[M\text{-}7CH_3]^+$.

ZnPcF$_8$SPyMe$_8$ 5a – mp: >300°C. ^{1}H NMR (DMSO-d_6): δ 4.22 (s, 24H, CH_3), 8.25 (d, J = 7.0, 16H, Py-*o*-H), 8.77 (d, J = 7.0, 16H, Py-*m*-H). ^{19}F NMR (DMSO-d_6): δ−127.24 (s, 8F, Pc-α-F). UV–Vis (DMSO) λ_{max} (log ε): 407 (4.46), 647 (4.29), 722 (4.84) nm. MS (MALDI-TOF) *m/z*: 1608.9 $[M\text{-}7CH_3]^+$.

Phthalocyanine solubility studies. The solubility of cationic phthalocyanines **3a**–**5a** in DMSO and PBS was assessed by UV–Visible spectroscopy. Concentrations, between 0.625 and 25 μmol·L^{-1}, obtained by the addition of aliquots of each phthalocyanine stock solution, were analyzed. The intensity of the Q-band *versus* phthalocyanine concentration was plotted in a graphic for linear regression to determine if these concentrations follow the Beer–Lambert law.

Photostability studies. The photobleaching rates of compounds **3a**–**5a** were determined by irradiating 2 mL of a diluted solution of each phthalocyanine in PBS (Abs ~1) under the same conditions used in the biological assays (150 mW·cm^{-2}). During their radiation the solutions were magnetically stirred and kept at room temperature. The concentration of the phthalocyanine derivative was quantified by visible absorption spectroscopy at regular time intervals. UV–Visible spectroscopy assessed the intensity of the Q-band at different intervals of time and the photostability was expressed as I_t/I_0 (%; I_t = intensity of the band at given time of irradiation, I_0 = intensity of the band before irradiation). Similar assays were performed in the dark to account for the effect of aggregation as a source of light-independent decay.

Singlet oxygen generation. The ability of the PS to generate singlet oxygen was qualitatively evaluated following the photooxidation of 3-diphenylisobenzofuran (DPBF), a singlet oxygen quencher (40). Stock solutions of each cationic phthalocyanine at 0.1 mmol·L^{-1} in DMF and a stock solution of DPBF at 10 mmol·L^{-1} in DMF/H_2O (9:1) were prepared. The reaction mixtures of 50 μmol·L^{-1} of DPBF and 0.5 μmol·L^{-1} of each phthalocyanine derivative in DMF/H_2O (9:1) were irradiated, in a glass cuvette at room temperature and under gentle magnetic stirring, with white light filtered through a cut-off filter for wavelengths <550 nm, at a fluence rate of 9.0 mW·cm^{-2}. The absorption decay of DPBF at 415 nm was measured at irradiation intervals of 1 up to 10 min. The percentage of the DPBF absorption decay, proportional to the production of $^1O_2$, was assessed by the difference between the initial absorbance and the absorbance of DPBF after a given period of irradiation.

Fluorescence quantum yield. The fluorescence quantum yields (Φ_F) of the phthalocyanine derivatives in DMF were measured in 1 × 1 cm quartz optical cells under normal air conditions on a spectrofluorimeter Fluoromax 3 (Horiba JovinYvon). The fluorescence quantum yields (Φ_F) of the phthalocyanine derivatives were calculated by comparison of the area below the corrected emission spectrum (600–800 nm) with that of phthalocyaninatozinc (II; ZnPc). ZnPc was used as fluorescence standard (λ_{exc} = 425 nm) with Φ_F = 0.28 in DMF (12). In all cases, the absorbance of the sample and reference solutions was kept at 0.02 at 425 nm, the excitation wavelength. Fluorescence quantum yield was calculated according equation (Eq. 1):

$$\Phi_F^{sample} = \Phi_F^{ref} \frac{AUC^{sample}(1 - 10^{-Abs_{ref}})}{AUC^{ref}(1 - 10^{-Abs_{sample}})} \quad (1)$$

where AUC is the integrated area under the fluorescence curves of each phthalocyanine and the standard and Abs is the absorbance of the samples and the standard at the excitation wavelength, respectively.

Bacterial culture. The bioluminescent *E. coli* strain used in this study was obtained in a previous study (41) and stored at −80°C in 10% glycerol. The *E. coli* Top10 (Invitrogen) was cloned with two plasmids as described by Maniatis *et al*. (42). These plasmids contain the lux operon from the bioluminescent marine bacterium *Vibrio fischeri*, required to produce light. The plasmid pHK724 contains a ColE1 replicon, an ampicillin resistance marker and *luxR* gene whose gene product is a transcription regulatory protein. The plasmid pHK555 contains a P15A replicon, a chloramphenicol resistance marker and a functional lux*ICDABE* operon. The *luxR* gene of pHK555 is inactive because of the insertion of phage DNA. When pHK724 is transformed into *E. coli* containing pHK555, the resultant colonies grow on selective media and are bioluminescent.

Before each photoinactivation assay, *E. coli* was aseptically spread-plated on TSA with the antibiotics ampicillin (100 mg·mL^{-1}) and chloramphenicol (25 mg·mL^{-1}) and grown for 1 day at 26°C. One isolated colony was aseptically inoculated on Luria Broth (LB; Merck) with both the antibiotics and grown overnight at 26°C under stirring (130 rpm). An aliquot (240 μL) of this culture was subcultured in LB (30 mL) with antibiotics and grown overnight under stirring (130 rpm) at 26°C.

Cellular uptake of phthalocyanines. A bacterial suspension (10^7 to 10^8 cells·mL^{-1}) was incubated for 10 min in the dark at room temperature in the presence of the same PS concentration used in the inactivation studies (20 μmol·L^{-1}). The unbound PS was removed out of the suspension by centrifugation at 13 000 ***g*** for 10 min (Eppendorf Microcentrifuge 5414). For the digestion, the pellets were resuspended in 1 mL of a digestion solution containing 0.5 mL of 2% aqueous SDS (Merck) and incubated at room temperature for at least 24 h. The concentration of the phthalocyanine derivatives in the digested extracts was analyzed by fluorimetry with a Fluoromax 3 (Horiba JovinYvon). The samples were excited at 425 nm and the fluorescence emission of the PS was monitored in the 440–900 nm range. The measured fluorescence intensity allowed the determination of the corresponding concentration by interpolation with a calibration plot built with known concentrations of each PS using the digestion solution as solvent. Parallel aliquots of the bacteria incubated in the presence of the PS were serially diluted and spread-plated in TSA for the determination of the concentration of viable *E. coli* (CFU·mL^{-1}). The adsorption value (PS CFU^{-1}) was calculated according to the literature (43). For each PS three independent assays were carried out.

Cellular localization of phthalocyanines. Bacterial cells (≈10^8 CFU · mL^{-1}) were incubated with each PS, as described in cellular uptake. After the incubation period, samples were centrifuged (12 000 ***g***, 6 min), and bacterial cells were washed twice with 1 mL of PBS to remove unbound PS. Cells were fixed with 4% paraformaldehyde in PBS for 30 min at room temperature. Cells were washed twice with 1 mL of PBS and permeabilized for 10 min in 500 μL of 0.1% Triton X-100 (Merck) in PBS, pH 7.4 at 50°C. The cells were washed twice with 1 mL of PBS, stained with the membrane marker FM1-43 (25 μmol·L^{-1}, Molecular Probes; Invitrogen) during 15 min at room temperature in the dark, washed twice with 1 mL of PBS. A 10 μL of glycerol were added to the pellet. Images of PS and FM1-43 fluorescence were acquired with a confocal microscope (Zeiss LSM 710). The preparation was excited at 488 nm and light emitted above 493 nm was collected for analysis of FM1-43. For analysis of the PS, each preparation was excited at 633 nm and emitted light was collected above 650 nm.

Correlation between bioluminescence and colony-forming units. To assess the correlation between the bioluminescent signal (in relative light units, RLU) of *E. coli* and the colony-forming units (CFU) number, two independent assays were carried out in dark conditions. A bioluminescent *E. coli* overnight culture (≈10^7 CFU·mL^{-1}) was serially diluted (10^{-1} to 10^{-7}) in PBS. The nondiluted and diluted aliquots were read on a luminometer (Turner Designs – 20/20) and pour plated in TSA medium. After 24 h of incubation at 37°C, the number of colonies was counted in the most convenient dilution series. Two independent assays were conducted.

Photoinactivation procedure. Bacterial cultures grown overnight were diluted 10-fold in PBS to a final concentration of ≈10^6 colony-forming units per milliliter (CFU mL^{-1}). This bacterial suspension was equally distributed in 100 mL sterilized and acid-washed glass beakers. Appropriate quantities of the three stock solution of the phthalocyanines derivatives **3a**–**5a** under study (500 μmol·L^{-1} DMSO) were added to achieve final concentrations of 20 μmol·L^{-1} (test sample) in a total volume of 10 mL per beaker. The samples were protected from light with aluminium foil and incubated for 10 min under 100 rpm stirring, at 25–30°C, to promote PS binding to *E. coli* cells. Light and dark controls were included in the experiments. The light control was

irradiated without phthalocyanine. The dark control contained 20 μmol·L^{-1} of phthalocyanine, but was protected from light with aluminium foil. Two independent assays were conducted for each condition.

Irradiation conditions. Following the preincubation period, the samples were irradiated with white light (400–800 nm) or red light (620–750 nm) delivered by an illumination system (LC-122 LumaCare, London) equipped with a halogen/quartz 250 W lamp coupled to two different interchangeable optic fiber probes (400–800 nm and 620–750 nm). The lights were delivered at a fluence rate of 150 mW·cm^{-2}, measured with an energy meter Coherent FieldMaxII-Top combined with a Coherent PowerSensPS19Q energy sensor. All samples were irradiated for 30 min under 100 rpm stirring, in a water bath at 25°C.

Bioluminescence monitoring. In all experiments, aliquots (50 μL^{-1}) of treated and control samples were collected at time 0 and after 2.5, 5, 10, 15, 20, 25 and 30 min of irradiation for bioluminescence measurement in a luminometer (TD-20/20 Luminometer; Turner Designs, Inc.).

Statistical analysis. Statistical analysis was performed with SPSS package (SPSS 15.0 for Windows, SPSS Inc.). Normal distributions were assessed by the Kolmogorov–Smirnov test. The significance of both irradiation time and type of PS on bacterial inactivation was assessed by two-way univariate analysis of variance (ANOVA) model with the Bonferroni *post hoc* test. A value of $P < 0.05$ was considered significant.

RESULTS

Synthesis of phthalocyanines and precursors

The synthetic routes used to prepare the novel cationic phthalocyanine derivates **3a**–**5a** are summarized in Scheme 1 and involved the previous preparation of the adequate neutral precursors **3**–**5**. The first two, **3** and **4** were prepared respectively from the tetramerization of phthalonitriles **1** and **2**, whereas **5** was prepared from the nucleophilic substitution of the eight beta fluor atoms of the synthetic available hexadecafluorophthalocyaninatozinc(II) by 4-mercaptopyridine. In both methodologies, the neutral precursors were isolated in yields higher than 80%.

The methylation of these metallophthalocyanines, carried out in the presence of a large excess of methyl iodide in DMF at 40°C afforded, after 16 h, followed by precipitation with diethyl ether, the cationic derivatives **3a**–**5a** quantitatively. The UV–Vis spectra of these phthalocyanines show the typical Soret and Q-bands, of beta substituted phthalocyanines (Fig. 1). In DMSO, the Q-bands of **3a–5a** present a bathochromic shift of ≈55 nm when compared with the same compounds in PBS. The broadening of the Q-bands and the appearance of two new bands in the Q-band regions of the metallophthalocyanine complexes in DMSO is suggestive of aggregation phenomena (44,45).

Phthalocyanine solubility

The phthalocyanines solubility in DMSO and PBS were measured by UV–Visible spectroscopy in concentrations between 0.625 and 25 μmol · L^{-1} to determine if the phthalocyanines, at this concentration range, follow the Beer–Lambert law. The graphics obtained from the plotting of the Q-band intensity *versus* phthalocyanine concentration in DMSO (Fig. 2) show a nonlinear regression for all the cationic phthalocyanines under study confirming that aggregation processes are occurring. A different situation occurs in PBS for compounds **3a** and **4a** at concentrations below 25 μmol · L^{-1} where the Beer–Lambert law is followed for both derivatives (Fig. 3). However, the behavior of phthalocyanine **5a** did not improve in PBS maintaining its high tendency to aggregate such as in DMSO.

Photostability, singlet oxygen generation and fluorescence quantum yield

The photostability studies showed that the three cationic compounds **3a**–**5a** when irradiated with white light or red light in PBS, under the same conditions used in the biological assays (30 min at a fluence rate of 150 mW·cm^{-2}), do not suffer pronounced changes in the residual absorbance (Table 1 and Fig. S1–S6), indicating that the new derivatives are photostable in the conditions used.

The results of the photooxidation of DPBF in the presence of the cationic phthalocyanines show that they are able to generate singlet oxygen, causing photodegradation of DPBF when irradiated with light at a fluence rate of 9 mW cm^{-2} (Table 1 and Fig. S7). However, the decay caused by tetra-substituted phthalocyanine **3a** was much higher (90% of DPBF decay after 5 min of irradiation) than those caused by the octa-substituted compounds (**4a**, **5a**), indicating a higher singlet oxygen rate production by this PS.

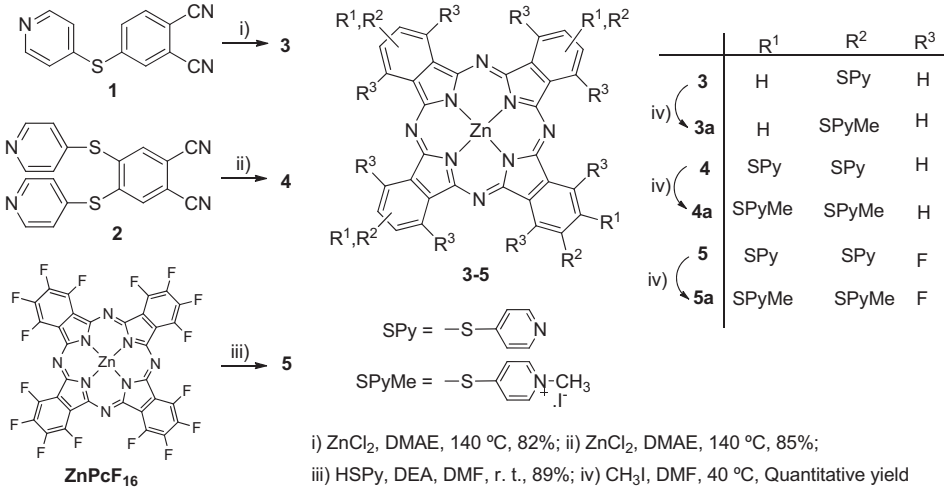

	R^1	R^2	R^3
3	H	SPy	H
3a	H	SPyMe	H
4	SPy	SPy	H
4a	SPyMe	SPyMe	H
5	SPy	SPy	F
5a	SPyMe	SPyMe	F

Scheme 1.

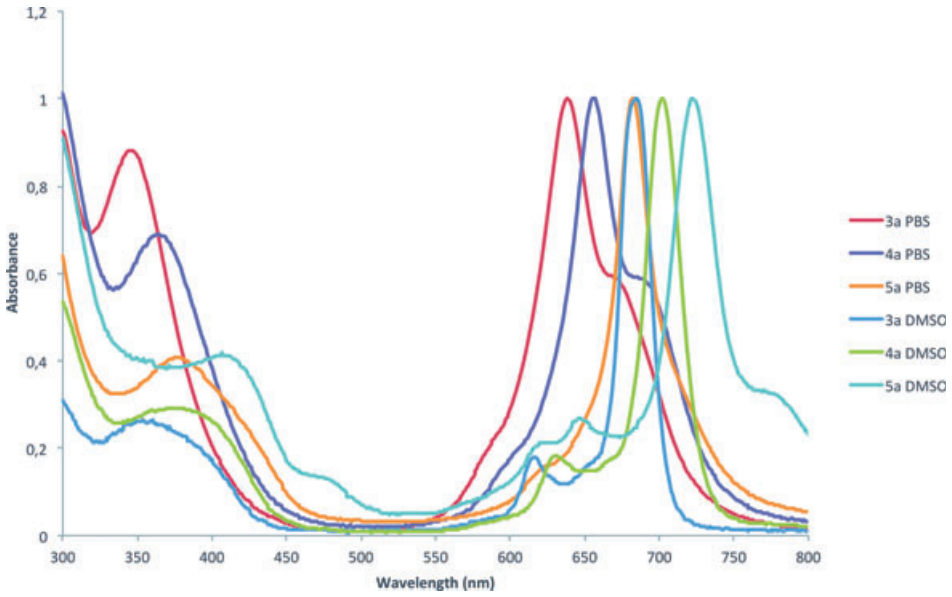

Figure 1. Normalized UV–Vis absorption spectra of phthalocyanines **3a–5a** in DMSO and PBS.

All new cationic derivatives were able to show fluorescence emission after excitation with visible light. In Table 1 are summarized the fluorescence quantum yields obtained for the derivatives **3a**–**5a** in DMF. According to the results obtained, compound **3a** (0.43) showed higher fluorescence quantum yield followed by compounds **4a** (0.25) and **5a** (0.16).

Cellular uptake of phthalocyanines

The values of cationic phthalocyanines uptake by the *E. coli*, obtained after 10 min of incubation in the dark at a concentration of 20 μmol·L^{-1}, and after two washings are summarized in Fig. 4. Compound **5a** showed the highest amount of phthalocyanine retention in *E. coli* cells, with an average value of 9.99×10^{21} molecules CFU^{-1}. The tetra-substituted phthalocyanine **3a** and the octa-substituted **4a** presented a similar uptake, with 5.24×10^{21} and 5.11×10^{21} molecules CFU^{-1}, respectively. The amount of phthalocyanine taken up by the bacterial cells decreased after each washing, and this decrease was more evident for **5a** (Fig. 4).

Cellular localization of phthalocyanines

The confocal immunofluorescence microscopy with FM1-43 as a membrane cell marker showed that all the compounds, even **5a** with a much higher uptake than **3a** and **4a**, have a similar behavior, with a uniform redistribution within the cell (Fig. 5).

Bioluminescence *versus* CFU of an overnight culture

The bioluminescence results reflect the bacterial abundance of the bioluminescent *E. coli* strain (Fig. 6). A significant linear correlation ($R^2 = 0.980$) was observed between bioluminescence units and colony counts.

Photoinactivation of bioluminescent *E. coli*

The results of the photoinactivation experiments show that the viability of the recombinant bioluminescent *E. coli* was not affected by light alone (light control) nor by the direct effect of any of the tested PS (dark controls; Fig. 7). Significant differences between the independent assays conducted for each phthalocyanine were not found (ANOVA, $P > 0.05$).

Comparing the bioluminescence values obtained in the experiments carried out under the white light (Fig. 7a), a clear difference in the photoinactivation patterns of the three phthalocyanines was observed. Compounds **3a** and **4a** were more efficient than **5a** ($P < 0.05$, ANOVA). The first two caused a 5 log (99.999% of reduction) decrease of bioluminescence after 30 min of irradiation, whereas the last one caused only 2.1 log reduction (≈99.33% of reduction). The experiments carried out under red light also showed different patterns of inactivation with the three PSs (Fig. 7b). The efficiency of photodynamic inactivation of **3a** was not very different from that obtained with white light (> 5 log decrease of bioluminescence) after 30 min of irradiation. However, the photodynamic inactivation with red light in the presence of compound **4a** was lower than that observed under white light (3.5 log decrease after 30 min of irradiation). In these conditions, compound **5a** was even less effective than under white light, causing 1 log decrease in bacterial bioluminescence.

DISCUSSION

The possibility of designing an enormous variety of structurally different phthalocyanines with high absorption in the red region of the electromagnetic spectrum places this class of second generation PSs among the most promising for the inactivation of pathogenic microorganisms in the clinic area. This fact supports the effort of several synthetic groups to obtain new derivatives based on phthalocyanines with improved features to be used as PS (30).

In this study an easy and efficient synthetic approach to obtain three new cationic phthalocyanines based on nucleophilic substitutions of commercial available precursors by 4-mercatopyridine is described. This selection was based on the knowledge that pyridine units after being quaternarized by

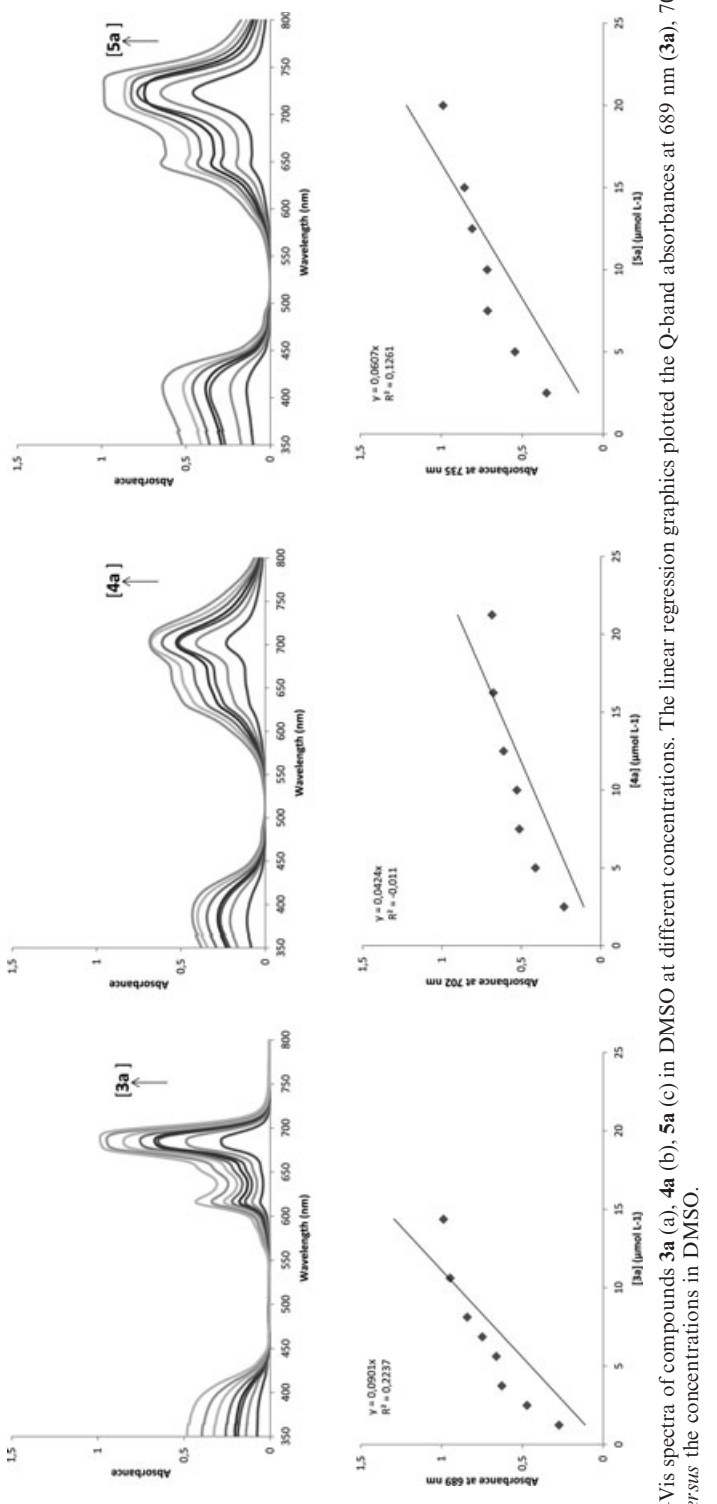

Figure 2. UV–Vis spectra of compounds **3a** (a), **4a** (b), **5a** (c) in DMSO at different concentrations. The linear regression graphics plotted the Q-band absorbances at 689 nm (**3a**), 702 nm (**4a**) and 725 nm (**5a**) *versus* the concentrations in DMSO.

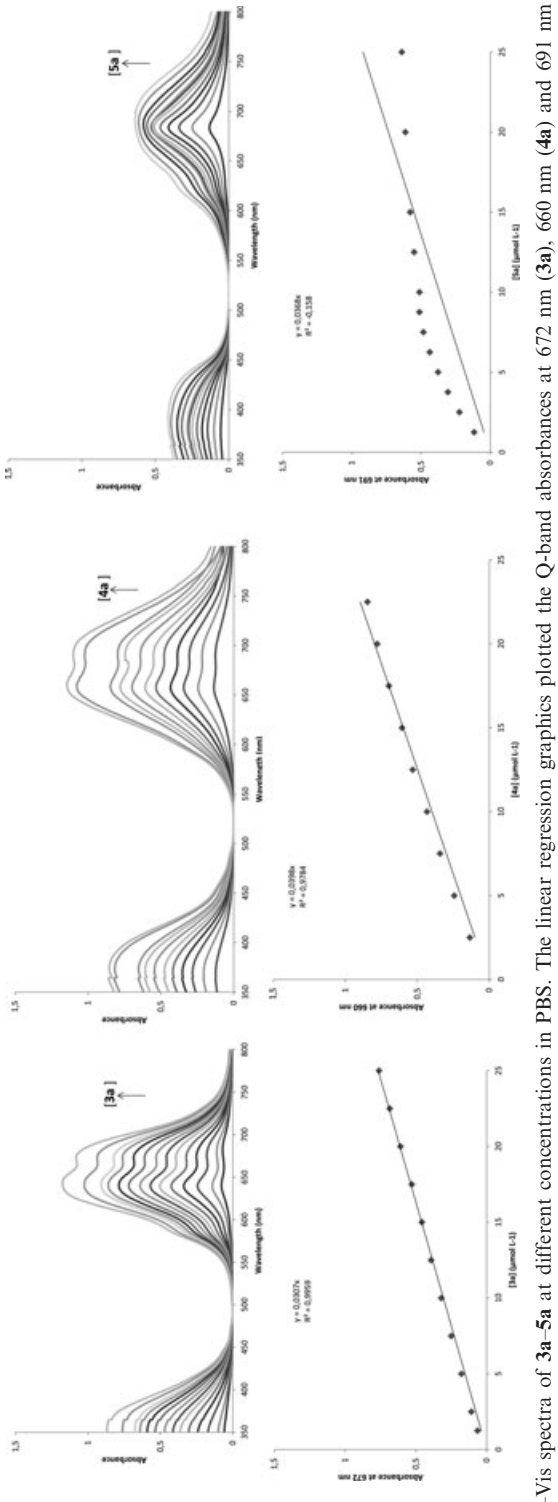

Figure 3. UV–Vis spectra of **3a**–**5a** at different concentrations in PBS. The linear regression graphics plotted the Q-band absorbances at 672 nm (**3a**), 660 nm (**4a**) and 691 nm (**5a**) *versus* the concentrations in PBS.

Table 1. Photostability, fluorescence quantum yield and relative photooxidation of DPBF by singlet oxygen generated by cationic phthalocyanine derivatives.

	Photostability (%)			
Compounds	White light*	Red light†	DPBF decay‡ (%)	Φ§
3a	90	90	90	0.43
4a	99	100	13	0.25
5a	97	99	11	0.16

*Upon 30 min of irradiation in PBS with white light (400–800 nm) at a fluence rate of 150 mW cm^{-2}. †Upon 30 min of irradiation in PBS with red light (620–750 nm) at a fluence rate of 150 mW cm^{-2}. ‡Upon 5 min of irradiation in DMF/H_2O (9:1) with white light filtered through a cutoff filter for wavelengths <550 nm, at a fluence rate of 9.0 mW cm^{-2}. §Reference ZnPc in DMF.

alkylation can confer an efficient antimicrobial photosensitizing activity (27). The neutral derivatives **3** and **4** were obtained respectively from the nucleophilic substitution of the 4-nitrophthalonitrile and 4,5-dichlorophthalonitrile with the selected pyridine derivative followed by the tetramerization step. Terivative **5** was obtained from the direct substitution, with the same nucleophile, of eight fluorine atoms from the commercially available hexadecafluorophthalocyaninatozinc (II). The neutral derivatives were obtained in yields higher than 80% and the methylation process allowed us to isolate the required cationic PS **3a**–**5a** quantitatively. This new series of derivatives with four (derivative **3a**) and eight charges (**4a** and **8a**) allows us to increase the number of cationic phthalocyanines with potentiality to be used as PS (11,12,24,37,38). The yields obtained in this study were higher than the ones referred to in literature for analogue derivatives (37,38; >80% *versus* 12%), and the compounds **4a** and **5a** were isolated as single compounds. Although cationic phthalocyanines (as a mixture of regioisomers) namely with eight charges were already reported in literature (11,24) and their efficiency as antibacterial PSs was evaluated, the charge was conferred by different groups from the ones studied here: trimethylammonium or anilinium *versus* pyridinium groups.

Considering the biological results this study shows that: (1) the three new cationic thio-pyridinium phthalocyanines with different physico-chemical properties have different photoinactivation efficiencies against a Gram-negative bacterium; (2) Phthalocyanines **3a** and **4a**, have high potential to be used as antimicrobial PSs under irradiation with white light (5 log reduction in *E. coli* bioluminescence); and (3) phthalocyanine **3a** is the most promising of the three PS under red light (5.5 log reduction in bioluminescence). The best performance of the tetra- and of the octa-substituted phthalocyanines **3a** and **4a,** when compared with the octa-substituted one **5a,** in the photoinactivation of Gram-negative bacteria can be explained by the tendency of **5a** to aggregate with consequent low $^1O_2$ production. The production of $^1O_2$ by phthalocyanine **3a** is approximately nine times higher than the octa-substituted **4a** and **5a**, probably due to the lower substitution of the Pc core by thiol groups. It is well known that $^1O_2$ can be quenched by thiols (46). According to the literature, $^1O_2$ is the main ROS through which the PS exerts their photodynamic action (47–50). Although the overall production of $^1O_2$ by **4a** is also reduced, the photoinactivation results show that it is still enough to photoinactivate efficiently the bacteria under white light. The low tendency of **4a** to aggregate can justify the different profile of the two-eight-positive charge PS.

The presence of one or more positively charged groups plays an essential role in driving the PS toward sites that are critical for the stability of cell organization and/or the cell functions (34,51,52). In fact, several studies demonstrate a high rate of bacterial inactivation with tri- and tetracationic porphyrinic PS compared with di- and monocationic molecules (31,52). However, other studies report on contradicting results (31,53) and it was even suggested that a high number of positive charges could decrease the PS efficiency (Jori, pers. comm.). These results are according to previously reported high PDI activity for tetra-cationic pyridinium zinc(II) phthalocyanine (PPc), a tetra-cationic methylpyridyloxy zinc(II) phthalocyanine and octa-cationic zinc(II) phthalocyanine bearing four bis(*N*,*N*,*N*-trimethyl)amino-2-propyloxy groups against *E. coli* (11,13,19).

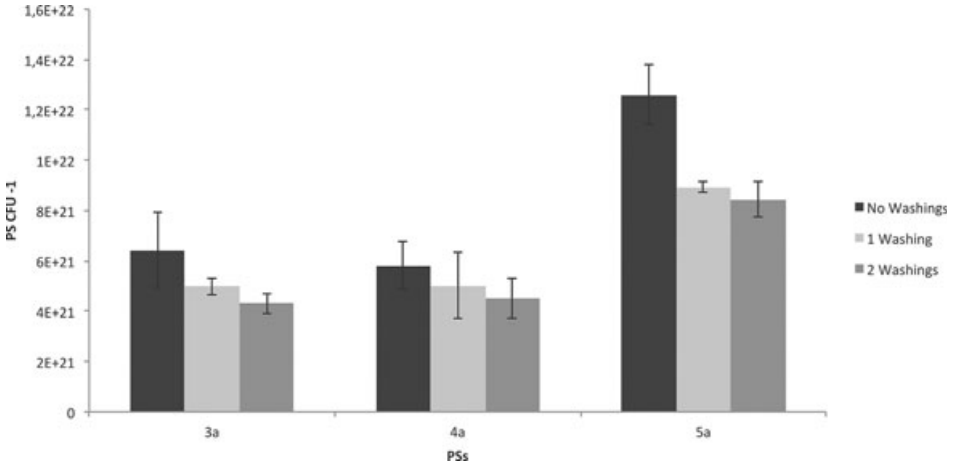

Figure 4. Adsorption of phthalocyanines **3a**–**5a** to *E. coli* in the presence of 20 $\mu mol \cdot L^{-1}$ of each PS, after incubation 10 min in the dark. Error bars represent the standard deviation.

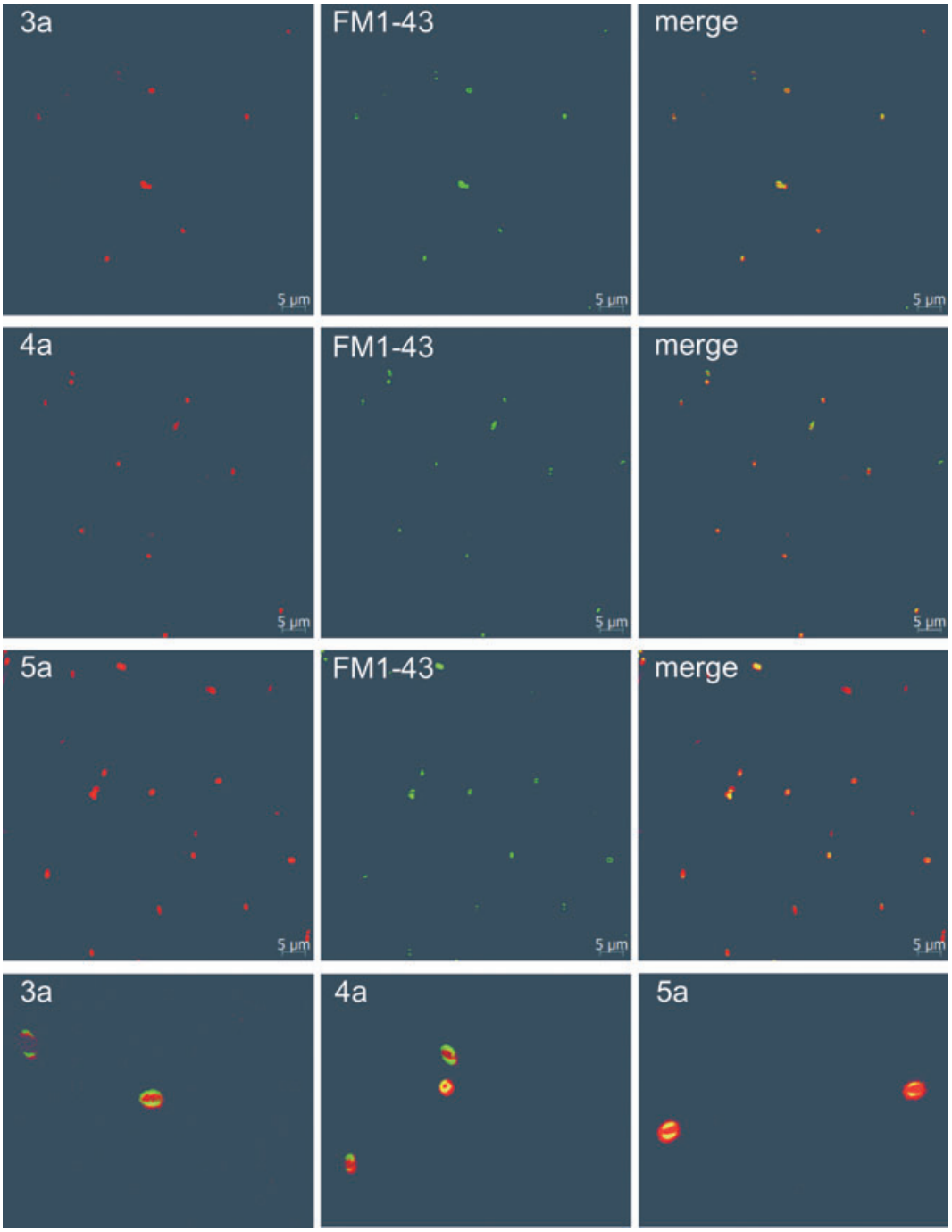

Figure 5. Confocal fluorescence microscopy images of *E. coli*, double stained with the PS (**3a**, **4a** and **5a**) and with the cell membrane marker, FM1-43. Right panels show the superimposed images from PS (red) and FM1-43 (green). The last row shows representative bacteria amplified from the merged images.

In this study, under white light, the tetra- (**3a**) and octa- (**4a**) show similar photoinactivation effect suggesting that the high number of positive charges does not affect PS efficiency.

All cationic compounds show higher photoinactivation efficiency under white light (400–800 nm) comparatively to red light (620–750 nm), most probably due to the higher overlap of the Q-bands with the emission spectrum of white light (see Fig. S8). The light wavelength necessary to induce microorganism photoinactivation depends on the electronic absorption spectrum of the PS, and the emission spectrum of the light source must cover all the PS absorption spectrum or at least some of the absorption bands (54). Under red light irradiation, the photoinactivation efficiency of PS **4a** was significantly lower ($P < 0.05$) than the one observed for **3a**. In this case, however, the overlap of the **3a** Q-band with the red light emission is lower than the corresponding **4a** Q-band overlap (see Fig. S8), the lower molar extinction coefficients of **4a** Q-band in that region can explain the much lower

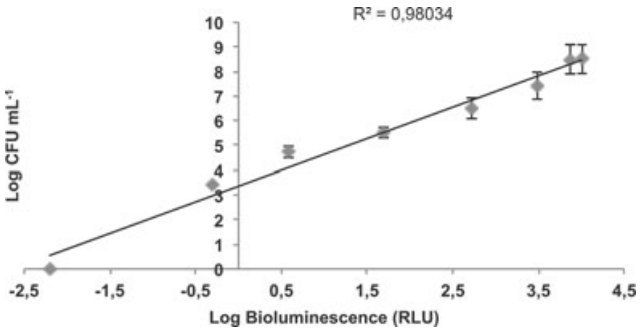

Figure 6. Linear correlation between the bioluminescence signal and colony counts of overnight cultures of recombinant bioluminescent *E. coli* serially diluted in PBS. Bacterial counts are expressed in CFU mL^{-1} and bioluminescence in relative light units (RLU). Each value represents average ± SD of two independent experiments.

production of $^1O_2$ due to less photons to be absorbed. The high photodynamic efficiency of compound **3a** under red light is of special interest considering potential clinical applications, because it penetrates deeper into human tissues than lower wavelengths (*e.g.* blue light).

Compound **5a** unexpectedly displayed the highest values of cellular adsorption. The compounds **3a** and **4a** showed similar uptake, although lower than **5a**. This suggests that the high uptake observed for **5a** is more likely an artifact related to aggregation in PBS. On the other hand, it has been shown that antibacterial photoinactivation is generally not dependent on surface-bound PS, but on the permeabilization of the cell membrane by reactive species produced by unbound PS molecules (55). Localization of the compounds may point out the sites of direct photodamage. Confocal microscopy images show that after 10 min incubation all compounds have an identical cellular localization.

CONCLUSION

Phthalocyanines **3a** and **4a** were prepared from pyridylphthalonitriles in very good yields. Phthalocyanine **5a** was also obtained, in good yields, *via* nucleophilic substitution of the fluor atoms of the hexadecafluorophthalocyaninatozinc(II) by 4-mercaptopyridine, followed by cationization.

The tetra-cationic phthalocyanine **3a** generates high amounts of singlet oxygen, which makes it an effective PS against *E. coli* reaching a 5 log reduction in bioluminescence emission after a 30 min of irradiation (total light dose 270 $J{\cdot}cm^{-2}$) with white light and 5.5 log under red light. Phthalocyanines with high amounts of thio-pyridinium groups showed a significant reduction in singlet oxygen generation; however, Pc **4a** under white light showed similar photoinactivation efficiency than the tetra-cationic Pc **3a**. Confocal immunofluorescence microscopy showed that phthalocyanines are uniformly distributed in the cell wall and within the cells. Under the studied conditions, compound **5a** did not show photoinactivation activity; however, the direct synthesis of Pc **5a**, from the commercial perfluorinated $ZnPcF_{16}$, can still justify the use of this template to prepare novel cationic PSs, eventually more active, if a different disposition/number from the combination used here, or if other cationic groups, rather than the pyridinium ones, were considered.

Acknowledgements—The authors would like to thank University of Aveiro, FCT (Portugal) and FEDER for funding the Organic Chemistry research unit QOPNA (project PEst-C/QUI/UI0062/2011), the associated laboratory CESAM, the Portuguese National NMR Network and the grant PTDC/QUI/65228/2006 to J. Tomé.

SUPPORTING INFORMATION

Additional Supporting Information may be found in the online version of this article:

Figure S1. Photostability of **3a** upon 30 min of irradiation in PBS with white light (400–800 nm) at a fluence rate of 150 mW cm^{-2}.

Figure S2. Photostability of **3a** upon 30 min of irradiation in PBS with red light (620–750 nm) at a fluence rate of 150 mW cm^{-2}.

Figure S3. Photostability of **4a** upon 30 min of irradiation in PBS with white light (400–800 nm) at a fluence rate of 150 mW cm^{-2}.

Figure S4. Photostability of **4a** upon 30 min of irradiation in PBS with red light (620–750 nm) at a fluence rate of 150 mW cm^{-2}.

Figure S5. Photostability of **5a** upon 30 min of irradiation in PBS with white light (400–800 nm) at a fluence rate of 150 mW cm^{-2}.

Figure S6. Photostability of **5a** upon 30 min of irradiation in PBS with red light (620–750 nm) at a fluence rate of 150 mW cm^{-2}.

Figure S7. Photooxidation of DPBF in the presence of the photosensitizers under study irradiated in DMF/H_2O (9:1)

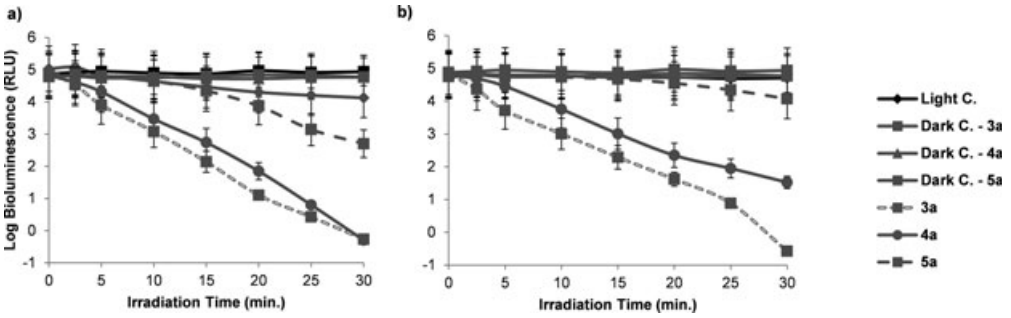

Figure 7. Photoinactivation bioluminescent *E. coli* in the presence of 20 μM of each PS under white light (a) or red light (b) at 150 $mW{\cdot}cm^{-2}$. Each value represents the average ± SD of two independent experiments.

with white light filtered through a cutoff filter for wavelengths < 550 nm, at a fluence rate of 9.0 mW cm^{-2}.

Figure S8. Normalized UV–Vis spectra of **3a**–**5a** in PBS and white and red light source emission.

Please note: Wiley-Blackwell is not responsible for the content or functionality of any supporting information supplied by the authors. Any queries (other than missing material) should be directed to the corresponding author for the article.

REFERENCES

1. Cassel, G. and J. Mekalanos (2001) Development of antimicrobial agents in the era of new and reemerging infectious diseases and increasing antibiotic resistance. *JAMA* **285**, 601–605.
2. Hamblin, M. and T. Hasan (2004) Photodynamic therapy: a new antimicrobial approach to infectious disease?. *Photochem. Photobiol. Sci.* **3**, 436–450.
3. O'Riordan, K., O. Akilov and T. Hasan (2005) The potential for photodynamic therapy in the treatment of localized infection. *Photodiagn. Photodyn. Ther.* **2**, 247–262.
4. Carvalho, C., A. Gomes, S. Fernandes, A. Prata, M. Almeida, M. Cunha, J. Tomé, M. Faustino, M. Neves, A. Tomé, J. Cavaleiro, Z. Lin, J. Rainho and J. Rocha (2007) Photoinactivation of bacteria in wastewater by porphyrins: bacterial β-galactosidase activity and leucine-uptake as methods to monitor the process. *J. Photochem. Photobiol., B* **88**, 112–118.
5. Jori, G. and S. Brown (2004) Photosensitized inactivation of microorganisms. *Photochem. Photobiol. Sci.* **3**, 403–405.
6. Ryakova, L., V. Buchta and R. Slezak (2010) Photodynamic antimicrobial therapy. *Cent. Eur. J. Biol.* **5**, 400–408.
7. Hasan, T. and J. A. Parrish (1997) Photodynamic therapy of cancer. In *Cancer Medicine* (Edited by J. F. Holland), pp. 739–751. Williams & Wilkins, Baltimore.
8. Maisch, T. (2007) Anti-microbial photodynamic therapy: useful in the future? *Lasers Med. Sci.* **22**, 83–91.
9. Cormick, M., M. Rovera and E. Durantini (2008) Synthesis, spectroscopic properties and photodynamic activity of a novel Zn(II) phthalocyanine substituted by fluconazole groups. *J. Photochem. Photobiol., A* **194**, 220–229.
10. Mantareva, V., V. Kussovski, I. Angelov, E. Borisova, L. Avramov, G. Schnurpfeil and D. Wöhrle (2007) Photodynamic activity of water-soluble phthalocyanine zinc(II) complexes against pathogenic microorganisms. *Bioorg. Med. Chem.* **15**, 4829–4835.
11. Segalla, A., C. D. Borsarelli, S. E. Braslavsky, J. D. Spikes, G. Roncucci, D. Dei, G. Chiti, G. Jori and E. Reddi (2002) Photophysical, photochemical and antibacterial photosensitizing properties of a novel octacationic Zn(II)-phthalocyanine. *Photochem. Photobiol. Sci.* **1**, 641–648.
12. Scalise, I. and E. Durantini (2005) Synthesis, properties, and photodynamic inactivation of *Escherichia coli* using a cationic and a noncharged Zn(II) pyridyloxyphthalocyanine derivatives. *Bioorg. Med. Chem.* **13**, 3037–3045.
13. Spesia, M., M. Rovera and E. Durantini (2010) Photodynamic inactivation of *Escherichia coli* and *Streptococcus mitis* by cationic zinc(II) phthalocyanines in media with blood derivatives. *Eur. J. Med. Chem.* **45**, 2198–2205.
14. Spiller, W., H. Kliesch, D. Wohrle, S. Hackbarth, B. Roder and G. Schnurpfeil (1998) Singlet oxygen quantum yields of different photosensitizers in polar solvents and micellar solutions. *J. Porphyrins Phthalocyanines* **2**, 145–158.
15. DeRosa, M. and R. Crutchley (2002) Photosensitized singlet oxygen and its applications. *Coord. Chem. Rev.* **233/234**, 351–371.
16. Moser, F. and A. Thomas. (1963) *Phthalocyanine Compounds*. Reinhold Publishing Corporation, New York.
17. Filippis, M. P., D. Dei, L. Fantetti and G. Roncucci (2000) Synthesis of a new water-soluble octa-cationic phthalocyanine derivative for PDT. *Tetrahedron Lett.* **41**, 9143–9147.
18. Claessens, C. G., U. Hahn and T. Torres (2008) Phthalocyanines: from outstanding electronic properties to emerging applications. *Chem. Rec.* **8**, 75–97.
19. Minnock, A., D. I. Vernon, J. Schofield, J. Griffiths, J. H. Parish and S. B. Brown (1996) Photoinactivation of bacteria. Use of a cationic water-soluble zinc phthalocyanine to photoinactivate both Gram-negative and Gram-positive bacteria. *J. Photochem. Photobiol., B* **32**, 159–164.
20. Bertoloni, G., F. Rossi, G. Valduga, G. Jori, H. Ali and J. E. van Lier (1992) Photosensitizing activity of water- and lipid-soluble phthalocyanines on prokaryotic and eukaryotic microbial cells. *Microbios* **71**, 33–46.
21. Reddi, E., C. Zhou, R. Biolo, E. Menegaldo and G. Jori (1990) Liposome- or LDL-administered Zn (II)-phthalocyanine as a photodynamic agent for tumours. I. Pharmacokinetic properties and phototherapeutic efficiency. *Br. J. Cancer* **61**, 407–411.
22. Valduga, G., E. Reddi, S. Garbisa and G. Jori (1998) Photosensitization of cells with diferente metastatic potentials by lyposome-delivered Zn(II)-phthalocyanine. *Int. J. Cancer* **75**, 412–417.
23. Josefsen, L. B. and R. W. Boyle (2008) Photodynamic therapy and the development of metal-based photosensitisers. *Met. Based Drugs* **2008**, 1–24.
24. Soncin, M., C. Fabris, A. Busetti, D. Dei, D. Nistri, G. Roncucci and G. Jori (2002) Approaches to selectivity in the Zn(II)-phthalocyanine-photosensitized inactivation of wild-type and antibiotic-resistant *Staphylococcus aureus*. *Photochem. Photobiol. Sci.* **1**, 815–819.
25. Atilla, D., M. Durmuş, A. G. Gürek, V. Ahsen and T. Nyokong (2007) Synthesis, photophysical and photochemical properties of poly(oxyethylene)-substituted zinc phthalocyanines. *Dalton Trans.* **28**, 1235–1243.
26. Yuksel, F., M. Durmuş and V. Ahsen (2011) Photophysical, photochemical and liquid crystalline properties of novel gallium(III) phthalocyanines. *Dyes Pigm.*, **90**, 191–200.
27. Jori, G., M. Camerin, M. Soncin, L. Guidolin, O. Coppellotti (2011) Antimicrobial photodynamic therapy: basic principles. In *Photodynamic Inactivation of Microbial Pathogens: Medical and Environmental Applications* (Edited by M. R. Hamblin and G. Jori), pp 1–18. Royal Society of Chemistry, Cambridge.
28. Wainwright, W. (2004) Photoantimicrobials—a PACT against resistance and infection. *Drug Future* **29**, 85–93.
29. Maisch, T., R.-M. Szeimies, G. Jori and C. Abels (2004) Antibacterial photodynamic therapy in dermatology. *Photochem. Photobiol. Sci* **3**, 907–917.
30. Nitzan, Y. and I. Pechatnikov (2011) Approaches to kill gram-negative bacteria by photosensitized processes. In *Photodynamic Inactivation of Microbial Pathogens: Medical and Environmental Applications* (Edited by M. R. Hamblin and G. Jori), pp 45–69. Royal Society of Chemistry, Cambridge.
31. Banfi, S., E. Caruso, L. Buccafurni, V. Battini, S. Zazzaron, P. Barbieri and V. Orlandi (2006) Antibacterial activity of tetraarylporphyrin photosensitizers: an *in vitro* study on Gram negative and Gram positive bacteria. *J. Photochem. Photobiol., B* **85**, 28–38.
32. Jori, G., C. Fabris, M. Soncin, S. Ferro, O. Coppellotti, D. Dei, L. Fantetti, G. Chiti and G. Roncucci (2006) Photodynamic therapy in the treatment of microbial infections: basic principles and perspective applications. *Lasers Surg. Med.* **38**, 468–481.
33. Denyer, S. and J. Maillard (2002) Cellular impermeability and uptake of biocides and antibiotics in Gram-negative bacteria. *J. Appl. Microbiol.* **92**, 35S–45S.
34. Merchat, M., G. Bertolini, P. Giacomini, A. Villanueva and G. Jori (1996) Meso-substituted cationic porphyrins as efficient photosensitizers of gram-positive and gram-negative bacteria. *J. Photochem. Photobiol., B* **32**, 153–157.
35. Soukos, N. S., L. A. Ximenez-Fyvie, M. R. Hamblin, S. S. Socransky and T. Hasan (1998) Targeted antimicrobial photochemotherapy. *Antimicrob. Agents Chemother.* **42**, 2595–2601.
36. Nitzan, Y. and H. Ashkenazi (2001) Photoinactivation of *Acinetobacterbaumannii* and *Escherichia coli* B by a cationic hydrophilic porphyrin at various light wavelengths. *Curr. Microbiol.* **42**, 408–414.
37. Saydan, N., M. Durmuş, M. G. Dizge, H. Yaman, A. G. Gürek, E. Antunes, T. Nyokong and V. Ahsen (2009) Water-soluble phthalocyanines mediated photodynamic effect on mesothelioma cells. *J. Porphyrins Phthalocyanines* **13**, 681–690.
38. Durmuş, M., H. Yaman, C. Göl, V. Ahsen and T. Nyokong (2011) Water-soluble quaternized mercaptopyridine-substituted zinc-phthalocyanines: synthesis, photophysical, photochemical and bovine serum albumin binding properties. *Dyes Pigm.* **91**, 153–163.

39. Armarego, W. L. F. and D. D. Perrin (1996) In: *Purification of Laboratory Chemicals*, 4th edn. Butterworth-Heinemann, Oxford.
40. Mitzel, F., S. FitzGerald, A. Beeby and R. Faust (2004) The synthesis of arylalkyne-substituted tetrapyrazinoporphyrazines and an evaluation of their potential as photosensitisers for photodynamic therapy. *Eur. J. Org. Chem.* **5**, 1136–1142.
41. Alves, E., C. Carvalho, J. Tomé, M. Faustino, M. Neves, A. Tomé, J. Cavaleiro, A. Cunha, S. Mendo and A. Almeida (2008) Photodynamic inactivation of recombinant bioluminescent *Escherichia coli* by cationic porphyrins under artificial and solar irradiation. *J. Ind. Microbiol. Biotechnol.* **35**, 1447–1454.
42. Maniatis, T., E. Fritsch and J. Sambrook (1989) *Molecular cloning: a laboratory manual*, Cold Spring Harbor Laboratory Press, Cold Spring Harbor, NY.
43. Demidova, T. N. and M. R. Hamblin (2005) Photodynamic inactivation of *Bacillus* spores, mediated by phenothiazinium dyes. *Appl. Environ. Microbiol.* **71**, 6918–6925.
44. Ogunsipe, A., D. Maree and T. Nyokong (2003) Solvent effects on the photochemical and fluorescence properties of zinc phthalocyanine derivatives. *J. Mol. Struct.* **650**, 131–140.
45. Nyokong, T. (2007) Effects of substituents on the photochemical and photophysical properties of main group metal phthalocyanines. *Coord. Chem. Rev.* **251**, 1707–1722.
46. Devasagayam, T. P., A. R. Sundquist, P. Di Mascio, S. Kaiser and H. Sies (1991) Activity of thiols as singlet molecular oxygen quenchers. *J. Photochem. Photobiol., B* **9**, 105–116.
47. Müller-Breitkreutz, K., H. Mohr, K. Briviba and H. Sies (1995) Inactivation of viruses by chemically and photochemically generated singlet molecular oxygen. *J. Photochem. Photobiol. B. Biol.* **30**, 63–70.
48. Ragàs, X., M. Agut and S. Nonell (2010) Singlet oxygen in *Escherichia coli*: new insights for antimicrobial photodynamic therapy. *Free Radical Bio. Med.* **49**, 770–776.
49. Nitzan, Y., B. Shainberg and Z. Malik (1989) The mechanism of photodynamic inactivation of *Staphylococcus aureus* by deuteroporphyrin. *Curr. Microbiol.* **19**, 265–269.
50. Maisch, T., R. M. Szeimies, N. Lehn and C. Abels (2005) Antibacterial photodynamic therapy. A new treatment for bacterial skin diseases? *Hautarzt* **56**, 1048–1055.
51. Lazzeri, D., M. Rovera, L. Pascual and E. N. Durantini (2004) Photodynamic studies and photoinactivation of *Escherichia coli* using meso-substituted cationic porphyrin derivatives with asymmetric charge distribution. *Photochem. Photobiol.* **80**, 286–293.
52. Caminos, D. A., M. B. Spesia and E. N. Durantini (2006) Photodynamic inactivation of *Escherichia coli* by novel meso-substituted porphyrins by 4-(3-*N,N,N*-trimethylammoniumpropoxy)phenyl and 4-(trifluoromethyl)phenyl groups. *Photochem. Photobiol. Sci.* **5**, 56–65.
53. Merchat, M., J. D. Spikes, G. Bertoloni and G. Jori (1996) Studies on the mechanism of bacteria photosensitization by *meso*-substituted cationic porphyrins. *J. Photochem. Photobiol., B* **35**, 149–157.
54. Costa, L., C. M. B. Carvalho, M. A. F. Faustino, M. G. P. M. S. Neves, J. P. C. Tomé, A. C. Tomé, J. A. S. Cavaleiro, A. Cunha and A. Almeida (2010) Sewage bacteriophage inactivation by cationic porphyrins: influence of light parameters. *Photochem. Photobiol. Sci.* **9**, 1126–1133.
55. Donnelly, R., P. McCarron and M. Tunney (2008) Antifungal photodynamic therapy. *Microbiol. Res.* **163**, 1–12.